PERGAMON

International Journal of Solids and Structures 37 (2000) 761–779

INTERNATIONAL JOURNAL OF SOLIDS and STRUCTURES

www.elsevier.com/locate/ijsolstr

A study of vibration of geometrically segmented beams with and without crack

T.D. Chaudhari, S.K. Maiti*

Department of Mechanical Engineering, Indian Institute of Technology, Bombay, Mumbai 400 076, India

Received 26 August 1998; in revised form 10 November 1998

Abstract

In this paper, a method of modelling for transverse vibrations of a geometrically segmented slender beam, with and without a crack normal to its axis, has been proposed using the Frobenius technique. There are two segments; one segment is uniform in depth and the other segment has a linearly variable depth. The thickness is uniform along the whole length. In the presence of a crack, the crack section is represented by a rotational spring. Thereby, it is possible to solve both the forward and inverse problems. In the forward problem, the frequencies can be determined by giving the rotational spring stiffness as an input. In the inverse problem, the method can be employed to detect the location and size of a crack by providing the natural frequencies as an input. A number of numerical examples are presented to demonstrate the accuracy of the method. Wherever possible, results have been compared with analytical solutions available in the literature. In the remaining cases, the results are found to be in very good agreement with finite element solutions. In the inverse problems, the error in prediction of crack location is less than 3% and that in size is around 25%. © 1999 Elsevier Science Ltd. All rights reserved.

Keywords: Cantilever; Crack; Euler–Bernoulli beam; Finite element; Vibration

1. Introduction

Beams of variable depth offer scope for a selective distribution of stiffness and weight. Sometimes, beams are composed of a variable and uniform depth segments; this may further help in fitting special functional requirements. The study of the vibration of such beams is very important, although not much attention has been focused on theoretical analysis so far. The lack of study is all the greater in the case

* Corresponding author. Tel.: +0091-22-576-7526; Fax: +0091-22-576-3480.
E-mail address: skmaiti@me.iitb.ernet.in (S.K. Maiti)

PII: S0020-7683(99)00054-2

of such beams with a crack; this has motivated the present study. The absence of any solution to the related inverse problem has been an additional factor for the motivation.

Auciello and Ercolano (1997) have analysed a geometrically two-segmented beam; one segment of the beam has a linearly varying depth and the other is of uniform depth. They have given a solution to the simply supported beams, etc., mainly based on the Bessel function approach.

Analysis of the vibration of a beam of smoothly varying depth or cross-section has been done by various investigators. Rao (1965) has used the Galerkin method to determine the fundamental frequency of a cantilever beam of linearly variable depth and thickness; he has compared the results with those of Martin (1956). Conway and Dubil (1965) have applied the Bessel function approach to examine beams of smoothly varying circular cross-section. Gaines and Volterra (1966) have given a procedure based on the Rayleigh–Ritz method to calculate the upper and lower bounds to the three lowest natural frequencies of transverse vibration of beams of variable depth and thickness. They have also considered beams of uniformly varying circular section and presented the influence of both rotary inertia and shear deformation.

Carnegie and Thomas (1967) have studied the behavior of a turbine or compressor blade by treating it as a taper beam of constant thickness. They have solved the related Euler–Bernoulli equation by the finite difference method. Wang (1967) has obtained solutions for a tapered beam of uniformly varying depth and thickness simultaneously in terms of generalized hypergeometric functions by the method of Frobenius. Mabie and Rogers (1968) have examined propped cantilever beams and solved the governing equation through numerical integration. They consider beams of either linearly variable depth or thickness. Naguleswaran (1994) has adapted the method of Frobenius to directly obtain solutions for wedge and cone beams. Therefore, there are not many solutions concerning beams of segmented configurations.

The problems of studying the vibration of beams become more involved in the presence of a crack or a crack-like defect. When a crack develops in a component, it leads to a change in its vibration parameters, e.g. stiffness, damping (Adams et al., 1975), etc. Some of these parameters have been shown to have potentials to serve as a basis to solve the inverse problem, i.e. to estimate the location and size of a crack in the beam (Rizos et al., 1990; Liang et al., 1991; Cawley and Adams, 1979; Dimarogonas, 1987) from its free vibration responses. Rizos et al. (1990) have proposed a method based on flexural vibration for uniform beams by representing the crack section by a rotational spring. The usefulness of the method for detection of both crack location and size is demonstrated for cantilever beams with normal edge cracks. The technique only needs measurement of the amplitudes at any two locations along the beam. Liang et al. (1991) have given a scheme which has a lot of similarity with that of Rizos et al., but it requires the measurement of three transverse natural frequencies of the beam. The method has been extended to stepped beams (Nandwana and Maiti, 1997a), beams on multiple supports (Nandwana and Maiti, 1997b), cantilever beams with inclined edge cracks (Nandwana and Maiti, 1997c), etc. There is a need to see if this approach can be adapted for a beam of segmented geometries and the inverse problem can be addressed.

The objective of this paper is therefore to present an analytical method for the study of transverse vibration of slender beam of constant thickness with and without cracks and made up of two segments, one of which has a linearly varying depth and the other is uniform. The method is based on the Frobenius technique. The effectiveness of method for both the forward and inverse problem is demonstrated through a number of numerical examples. Both cantilever and simply supported boundary conditions are considered. The beams studied are slender beams (of slenderness ratio in the range 12 to 24) of isotropic material. For this range of slenderness ratio, the effects of rotational inertia and shear deformation can be neglected. Consequently, the mode I SIF will have the dominant role in the prediction of the location and size of a crack.

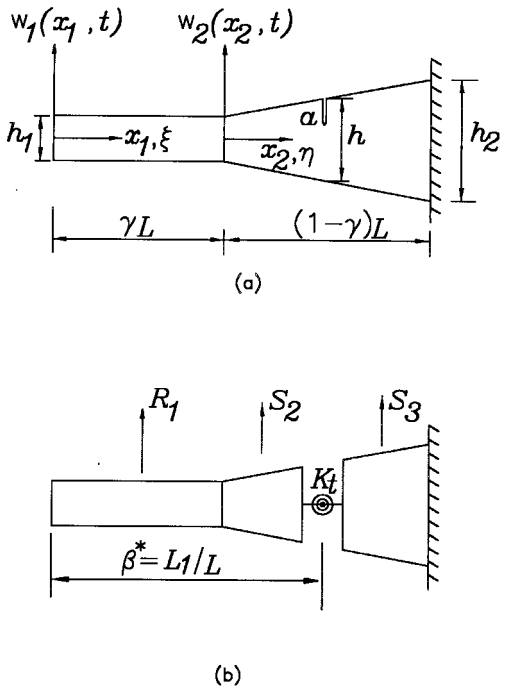

Fig. 1. (a) Actual beam geometry; (b) crack representation by rotational spring.

2. Formulation

For a slender beam with two different geometric segments (Fig. 1), the associated displacement functions, $w_1(x_1,t)$ and $w_2(x_2,t)$, can be written in the form

$$w_1(x_1,t) = R(x_1)e^{i\omega t},\ 0 \le x_1 \le \gamma L$$

$$w_2(x_2,t) = S(x_2)e^{i\omega t},\ 0 \le x_2 \le (1-\gamma)L,$$

where γ is the length truncation factor and $R(x_1)$ and $S(x_2)$ are the mode shapes.

The governing equations of motion, neglecting the rotational inertia and shear deformation, can be converted into the well-known Euler–Bernoulli equations:

$$EI_1\frac{d^4R}{dx_1^4} - \rho A_1\omega^2 R = 0,\ 0 \le x_1 \le \gamma L, \tag{1}$$

$$\frac{d^2}{dx_2^2}\left[EI_{x_2}\frac{d^2S}{dx_2^2}\right] - \rho A_{x_2}\omega^2 S = 0,\ 0 \le x_2 \le (1-\gamma)L, \tag{2}$$

where E is modulus of elasticity, ρ is density, I_1 and A_1 are moment of inertia and area at small end, I_{x_2}

and A_{x_2} are moment of inertia and area at any location of the linearly variable depth segment. Introducing the dimensionless parameters,

$$\xi = \frac{x_1}{L}$$

$$\eta = \left[1 + \frac{(1-\alpha)}{\alpha(1-\gamma)} x_2\right],$$

where $\alpha = (h_1/h_2)$ is a height truncation factor. A_{x_2} and I_{x_2} can be expressed as

$$A_{x_2} = \eta A_1$$

$$I_{x_2} = \eta^3 I_1.$$

It may be noted that the dimensionless parameters introduced here are different from those of Naguleswaran (1994).

Eqs. (1) and (2) can be converted to the following convenient non-dimensional forms:

$$\frac{\mathrm{d}^4 R(\xi)}{\mathrm{d}\eta^4} - p^4 R(\xi) = 0, \quad 0 \le \xi \le \gamma \tag{3}$$

$$\eta^2 \frac{\mathrm{d}^4 S(\eta)}{\mathrm{d}\eta^4} + 6\eta \frac{\mathrm{d}^3 S(\eta)}{\mathrm{d}\eta^3} + 6\frac{\mathrm{d}^2 S(\eta)}{\mathrm{d}\eta^2} - q_\alpha^4 S(\eta) = 0, \quad 1 \le \eta \le \frac{1}{\alpha}, \tag{4}$$

where

$$p^4 = \frac{\rho A_1 L^4 \omega^2}{E I_1}, \quad q_\alpha = p\left(\frac{1-\gamma}{1-\alpha}\right)\alpha.$$

2.1. Direct solution for uncracked beam

The solution of Eq. (3) can be expressed as

$$R(\xi) = A_1 \cosh p\xi + A_2 \cos p\xi + A_3 \sinh p\xi + A_4 \sin p\xi, \tag{5}$$

where A_1, A_2, A_3 and A_4 are arbitrary constants.

Since Eq. (4) for the tapered segment is a fourth order differential equation, its general solution can be written in terms of four linearly independent solutions. These can be determined through the method of Frobenius. The trial solution can be written in the form of a power series

$$S(\eta, C) = \sum_{n=0}^{\infty} a_{n+1}(C)\eta^{C+2n} = a_1(C)\eta^C + a_2(C)\eta^{C+2} + \ldots, \tag{6}$$

where C is an undetermined exponent. Substituting $S(\eta,C)$ as $S(\eta)$ in Eq. (4):

$$(C+1)C^2(C-1)a_1(C)\eta^{C-2}+\Big[(C+3)(C+2)^2(C+1)a_2(C)-q_\alpha^4 a_1(C)\Big]\eta^C+$$
$$\sum_{n=0}^{\infty}\Big[(C+2n+5)(C+2n+4)^2(C+2n+3)a_{n+3}(C)-q_\alpha^4 a_{n+2}(C)\Big]\eta^{C+2n+2}=0. \tag{7}$$

Since the right hand side is 0, the coefficients of all the exponential terms must vanish. This gives

$$(C+1)C^2(C-1)a_1(C)=0,$$

$$a_1(C)=(C+3)(C+2)^2(C+1)a_2(C)\big/q_\alpha^4 \tag{8}$$

$$(C+2n+5)(C+2n+4)^2(C+2n+3)a_{n+3}(C)-q_\alpha^4 a_{n+2}(C)=0 \tag{9}$$

for $n = 0,1,2,\ldots, \infty$.

If $a_2(C)$ is assumed to be 0, then all other constants, $a_1(C)$, $a_3(C)$, etc., become zero. This therefore gives the trivial solution. For a nontrivial solution, $a_2(C)$ is taken as 1 and the other constants, $a_3(C)$, $a_4(C)$, $a_5(C)$, etc., are obtained in terms of C through the recurrence relations. Finally, $S(\eta,C)$ has the form

$$S(\eta,C)=(C+3)(C+2)^2(C+1)\eta^C\big/q_\alpha^4+\eta^{C+2}+\sum_{n=0}^{\infty}a_{n+3}(C)\eta^{C+2n+4}. \tag{10}$$

Again, on substitution of $S(\eta,C)$ as $S(\eta)$ in Eq. (4),

$$\eta^2\frac{\mathrm{d}^4S(\eta,C)}{\mathrm{d}\eta^4}+6\eta\frac{\mathrm{d}^3S(\eta,C)}{\mathrm{d}\eta^3}+6\frac{\mathrm{d}^2S(\eta,C)}{\mathrm{d}\eta^2}-q_\alpha^4S(\eta,C)=(C+3)(C+2)^2(C+1)^2C^2(C-1)\frac{\eta^{C-2}}{q_\alpha^4}. \tag{11}$$

For $S(\eta,C)$ to be a solution of Eq. (4), the left hand side of Eq. (11) ought to be zero. Therefore

$$(C+3)(C+2)^2(C+1)^2C^2(C-1)=0. \tag{12}$$

This gives the possible values of C: $C = 0, 0, 1, -3, -2, -1, -2$. For $C=-3$, it is seen from Eqs. (8) and (9) that $a_{n+3}(C)$ becomes singular. Hence this value of C is not acceptable. Solutions $S(\eta,C)$ corresponding to $C=-2$ and $C = 0$ are linearly related. The same type of situation arises for $C=-1$ and $C=+1$. So, only the roots $C=-1$ and $C=-2$ are free of any such problems and are acceptable. The two independent mode shapes, which corresponds to $C=-1$ and $C=-2$, are given by

$$S(\eta,-1)=\eta+\frac{q_\alpha^4\eta^3}{4.3^2.2}+\frac{q_\alpha^8\eta^5}{6.5^2.4.4.3^2.2}+\cdots \tag{13}$$

$$S(\eta,-2)=1+\frac{q_\alpha^4\eta^2}{3.2^2.1}+\frac{q_\alpha^8\eta^4}{5.4^2.3.3.2^2.1}+\ldots. \tag{14}$$

These are the first and second solutions of the mode shape Eq. (4).

The third and fourth solutions are determined by following the further steps of the Frobenius method. By differentiating both sides of Eq. (11) with respect to C, the following equation is obtained.

$$\eta^2\frac{\mathrm{d}^4}{\mathrm{d}\eta^4}\left(\frac{\partial S(\eta,C)}{\partial C}\right)+6\eta\frac{\mathrm{d}^3}{\mathrm{d}\eta^3}\left(\frac{\partial S(\eta,C)}{\partial C}\right)+6\frac{\mathrm{d}^2}{\mathrm{d}\eta^2}\left(\frac{\partial S(\eta,C)}{\partial C}\right)-q_\alpha^4\left(\frac{\partial S(\eta,C)}{\partial C}\right)=$$
$$\frac{\partial}{\partial C}\left[(C+3)(C+2)^2(C+1)^2C^2(C-1)\frac{\eta^{C-2}}{q_\alpha^4}\right]. \tag{15}$$

The right hand side vanishes when $C=0,-1,-2$. Therefore, it is obvious that $\partial S(\eta,\mathrm{C})/\partial C|_{C=-1}$ and $\partial S(\eta,C)/\partial C|_{C=-2}$ are also solutions of Eq. (4). Explicitly

$$\frac{\partial S(\eta,C)}{\partial C}=[(C+3)(C+2)(2C+3)+(C+2)(C+1)(2C+5)]\frac{\eta^C}{q_\alpha^4}+(C+3)(C+2)^2(C+1)\eta^C$$
$$\frac{\ln\eta}{q_\alpha^4}+\eta^{C+2}\ln\eta+\sum_{n=0}^{\infty}a_{n+3}(C)\eta^{C+2n+4}\varphi_{n+3}(\eta,C), \tag{16}$$

where

$$\varphi_{n+3}(\eta,C)=\varphi_{n+2}(\eta,C)-\frac{1}{C+2n+5}-\frac{2}{C+2n+4}-\frac{1}{C+2n+3}$$

$$\varphi_2(\eta,C)=\ln\eta.$$

In particular, for $n=0$

$$\varphi_3(\eta,C)=\varphi_2(\eta,C)-\frac{1}{C+5}-\frac{2}{C+4}-\frac{1}{C+3}.$$

Substituting $C=-1$ and $C=-2$ in Eq. (16), the other two solutions, say $S^*(\eta,-1)$ and $S^*(\eta,-2)$, are obtained. That is,

$$\frac{\partial S(\eta,-1)}{\partial C}=S^*(\eta,-1)=(2.1)\frac{\eta^{-1}}{q_\alpha^4}+\eta\ln\eta+\left[\frac{q_\alpha^4\eta^3}{4.3^2.2}\right]\left[\ln\eta-\frac{1}{4}-\frac{2}{3}-\frac{1}{2}\right]+\ldots \tag{17}$$

$$\frac{\partial S(\eta,-2)}{\partial C}=S^*(\eta,-2)=\ln\eta+\left[\frac{q_\alpha^4\eta^2}{3.2^2.1}\right]\left[\ln\eta-\frac{1}{3}-\frac{2}{2}-\frac{1}{1}\right]+\ldots. \tag{18}$$

These two solutions are linearly independent and are, therefore, the required third and fourth solutions. Hence, the general solution of the mode shape Eq. (4) can now be written:

$$S(\eta) = B_1 S(\eta, -1) + B_2 S(\eta, -2) + B_3 S^*(\eta, -1) + B_4 S^*(\eta, -2). \tag{19}$$

The eight arbitrary constants A_1, A_2, A_3, A_4, B_1, B_2, B_3 and B_4 involved in Eqs. (5) and (19) are obtained from the four boundary conditions and four continuity conditions at the junction of the two segments. The continuity conditions are in terms of displacement, slope, shear force and moments.

3. Formulation for beam with crack

For a beam with a crack, the beam can be split into three segments (Fig. 1) and the mode shape equation for each segment can be written separately. The segments lying on either side of the crack are considered to be connected by a rotational spring (Liang et al., 1991). The solutions for the three segments can be written as follows:

$$R_1(\xi) = A_{11} \cosh p\xi + A_{12} \cos p\xi + A_{13} \sinh p\xi + A_{14} \sin p\xi$$

for the uniform depth segment,

$$S_2(\eta) = A_{21} S_2(\eta, -1) + A_{22} S_2(\eta, -2) + A_{23} S_2^*(\eta, -1) + A_{24} S_2^*(\eta, -2)$$

for the taper segment lying on the left of the crack and

$$S_3(\eta) = A_{31} S_3(\eta, -1) + A_{32} S_3(\eta, -2) + A_{33} S_3^*(\eta, -1) + A_{34} S_3^*(\eta, -2)$$

for the taper segment lying to the right of the crack.

The condition of continuity of displacement, moment and shear forces at the crack location (say, $\eta = \beta^* = L_1/L$) and jump in the slope at the crack section are respectively given by:

$$S_2(\eta) = S_3(\eta) \tag{20}$$

$$\frac{\mathrm{d}^2 S_2(\eta)}{\mathrm{d}\eta^2} = \frac{\mathrm{d}^2 S_3(\eta)}{\mathrm{d}\eta^2}, \tag{21}$$

$$\left(3\frac{\mathrm{d}^2 S_2(\eta)}{\mathrm{d}\eta^2} + \frac{\mathrm{d}^3 S_2(\eta)}{\mathrm{d}\eta^3}\right) = \left(3\frac{\mathrm{d}^2 S_3(\eta)}{\mathrm{d}\eta^2} + \frac{\mathrm{d}^3 S_3(\eta)}{\mathrm{d}\eta^3}\right) \tag{22}$$

$$\frac{\mathrm{d}S_2(\eta)}{\mathrm{d}\eta} + \frac{1}{K}\frac{\mathrm{d}^2 S_2(\eta)}{\mathrm{d}\eta^2} = \frac{\mathrm{d}S_3(\eta)}{\mathrm{d}\eta}, \tag{23}$$

where $K = (K_t L/EI_1)$ is the non-dimensional stiffness of the rotational spring. The compatibility conditions of displacement, slope, moment and shear force at the junction of two geometric segments (i.e. at $\xi = \gamma$ or $\eta = 1$) are

$$R_1(\xi) = S_2(\eta), \tag{24}$$

$$\frac{\mathrm{d}R_1(\xi)}{\mathrm{d}\xi} = \left(\frac{1-\alpha}{\alpha(1-\gamma)}\right)\frac{\mathrm{d}S_2(\eta)}{\mathrm{d}\eta}, \tag{25}$$

$$\frac{\mathrm{d}^2 R_1(\xi)}{\mathrm{d}\xi^2} = \left(\frac{1-\alpha}{\alpha(1-\gamma)}\right)^2 \frac{\mathrm{d}^2 S_2(\eta)}{\mathrm{d}\eta^2} \tag{26}$$

$$\frac{\mathrm{d}^3 R_1(\xi)}{\mathrm{d}\xi^3} = \left(\frac{1-\alpha}{\alpha(1-\gamma)}\right)^3 \left(\frac{\mathrm{d}^3 S_2(\eta)}{\mathrm{d}\eta^3} + 3\frac{\mathrm{d}^2 S_2(\eta)}{\mathrm{d}\eta^2}\right). \tag{27}$$

The boundary conditions are given by

$$S_3(\eta) = 0 \text{ and } \frac{\mathrm{d}S_3(\eta)}{\mathrm{d}\eta} = 0 \text{ for } \eta = \frac{1}{\alpha} \text{ (i.e. at the fixed end)}, \tag{28}$$

$$\frac{\mathrm{d}^2 R(\xi)}{\mathrm{d}\xi^2} = 0 \text{ and } \frac{\mathrm{d}^3 R(\xi)}{\mathrm{d}\xi^3} = 0 \text{ for } \xi = 0 \text{ (i.e. at the free end)}. \tag{29}$$

These 12 conditions are sufficient to solve for the 12 arbitrary constants. The equations involving these constants can be written in the form

$$[H]\{A\} = \{0\}, \tag{30}$$

where $\{A\}$ is the vector of the 12 arbitrary constants A_{ij} and the coefficient matrix $[H]$ is of dimension 12×12 and is given by:

$$[H] = \begin{bmatrix} [B_{FR}] & [0] & [B_{FX}] \\ [M_j] & [M_2] & [M_3] \\ [S_1] & [S_2] & [S_3] \end{bmatrix}. \tag{31}$$

When the crack is located in the taper segment, $[S_1]$ and $[M_3]$ will be null matrices of size 4×4. The non-zero submatrices of $[H]$ are of dimensions 4×4 and explicitly given by

$$[B_{FR}] = \begin{bmatrix} 1 & -1 & 0 & 0 \\ 0 & 0 & 1 & -1 \\ 0 & 0 & 0 & 0 \\ 0 & 0 & 0 & 0 \end{bmatrix},$$

$$[B_{FX}] = \begin{bmatrix} 0 & 0 & 0 & 0 \\ 0 & 0 & 0 & 0 \\ S_3\left(\frac{1}{\alpha}, -1\right) & S_3\left(\frac{1}{\alpha}, -2\right) & S_3^*\left(\frac{1}{\alpha}, -1\right) & S_3^*\left(\frac{1}{\alpha}, -2\right) \\ DS_3\left(\frac{1}{\alpha}, -1\right) & DS_3\left(\frac{1}{\alpha}, -2\right) & DS_3^*\left(\frac{1}{\alpha}, -1\right) & DS_3^*\left(\frac{1}{\alpha}, -2\right) \end{bmatrix}, \tag{32}$$

$$[M_j] = \begin{bmatrix} \cosh p\gamma & \cos p\gamma & \sinh p\gamma & \sin p\gamma \\ p\sinh p\gamma & -p\sin p\gamma & p\cosh p\gamma & p\cos p\gamma \\ p^2\cosh p\gamma & -p^2\cos p\gamma & p^2\sinh p\gamma & -p^2\sin p\gamma \\ p^3\sinh p\gamma & p^3\sin p\gamma & p^3\cosh p\gamma & -p^3\cos p\gamma \end{bmatrix}, \tag{33}$$

$$[M_i] = \begin{bmatrix} S_i(1,-1) & S_i(1,-2) & S_i^*(1,-1) & S_i^*(1,-2) \\ \mu D S_i(1,-1) & \mu D S_i(1,-2) & \mu D S_i^*(1,-1) & \mu D S_i^*(1,-2) \\ \mu^2 D^2 S_i(1,-1) & \mu^2 D^2 S_i(1,-2) & \mu^2 D^2 S_i^*(1,-1) & \mu^2 D^2 S_i(1,-2) \\ \mu^3\{D^3 S_i(1,-1) + 3D^2 S_i(1,-1)\} & \mu^3\{D^3 S_i(1,-2) + 3D^2 S_i(1,-2)\} & \mu^3\{D^3 S_i^*(1,-1) + 3D^2 S_i^*(1,-1)\} & \mu^3\{D^3 S_i^*(1,-2) + 3D^2 S_i^*(1,-2)\} \end{bmatrix} \tag{34}$$

for $i = 2,3$, $D = \mathrm{d}/\mathrm{d}\eta$ and $\mu = (1-\alpha)/[\alpha(1-\gamma)]$,

$$[S_i] = \begin{bmatrix} S_i(\beta,-1) & S_i(\beta,-2) & S_i^*(\beta,-1) & S_i^*(\beta,-2) \\ D^2 S_i(\beta,-1) & D^2 S_i(\beta,-2) & D^2 S_i^*(\beta,-1) & D^2 S_i^*(\beta,-2) \\ \{3D^2 S_i(\beta,-1) + D^3 S_i(\beta,-1)\} & \{3D^2 S_i(\beta,-2) + D^3 S_i(\beta,-2)\} & \{3D^3 S_i^*(\beta,-1) + D^3 S_i^*(\beta,-1)\} & \{3D^3 S_i^*(\beta,-2) + D^3 S_i^*(\beta,-2)\} \\ \{KDS_i(\beta,-1) + \mu D^2 S_i(\beta,-1)\} & \{KDS_i(\beta,-2) + \mu D^2 S_i(\beta,-2)\} & \{KDS_i^*(\beta,-1) + \mu D^2 S_i^*(\beta,-1)\} & \{KDS_i^*(\beta,-2) + \mu D^2 S_i^*(\beta,-2)\} \end{bmatrix} \tag{35}$$

for $i = 2$ and 3.

When a crack is located in the uniform depth segment of the beam, Eq. (31) has the same form, except that $[M_2]$ is exchanged with $[M_j]_{\gamma=\beta}$ and $[M_j]$ becomes a null matrix. Also,

$$[S_3] = [0]$$

$$[S_1] = [M_j]_{\gamma=\beta} = [S_2].$$

The characteristics equation of vibration is determinant $[H]=0$, i.e. $|H|=0$. The characteristic equation can be written in the form

$$K = -\frac{|\Delta_2|}{|\Delta_1|}. \tag{36}$$

By following similar steps, the characteristic equation for the beam when the crack is located in the uniform depth segment can also be obtained. This equation can be rearranged to give

$$K = -q_\alpha^4 \frac{|\Delta_2|}{|\Delta_1|}. \tag{37}$$

In Eq. (36), $|\Delta_1|$ and $|\Delta_2|$ have the same form as $|H|$ except for the last rows. The last row of $|\Delta_1|$ is given by

$$\begin{array}{llll} |DS_2(\beta,-1) & DS_2(\beta,-2) & DS_2^*(\beta,-1) & DS_2^*(\beta,-2) \\ -DS_3(\beta,-1) & -DS_3(\beta,-2) & -DS_3^*(\beta,-1) & -DS_3^*(\beta,-2) \\ 0 & 0 & 0 & 0| \end{array}$$

and the last row of $|\Delta_2|$ is given by

$$|D^2S_2(\beta,-1) \quad D^2S_2(\beta,-2) \quad D^2S_2^*(\beta,-1) \quad D_2S_2^*(\beta,-2) \quad 0 \quad 0 \quad 0 \quad 0 \quad 0 \quad 0 \quad 0 \quad 0|$$

Similarly, $|\Delta_1|$ and $|\Delta_2|$ in Eq. (37) have the same form as $|H|$ except for the last rows. The last row of $|\Delta_1|$ is given by

$$\begin{array}{llllllll} |\sinh p\beta & -\sin p\beta & \cosh p\beta & \cos p\beta & -\sinh p\beta & \sin p\beta & -\cosh p\beta & -\cos p\beta \\ 0 & & 0 & & 0 & & 0| & \end{array}$$

and the last row of $|\Delta_2|$ is given by

$$|\cosh p\beta \quad -\cos p\beta \quad \sinh p\beta \quad -\sin p\beta \quad 0 \quad 0 \quad 0 \quad 0 \quad 0 \quad 0 \quad 0 \quad 0|.$$

4. Numerical studies

4.1. Solution of forward problem

The method of solution has been tested considering both uncracked and cracked beams. The first geometric combination considered includes: Length $(L)=480$ mm, thickness $=12$ mm and depth at the fixed end $(h_2)=20$ mm, depth at free end $(h_1)=8$ mm, length of taper section $=240$ mm and length of uniform section $=240$ mm. The height truncation factor, α, is 0.4 and length truncation factor, γ, is 0.5. The case, $\gamma=0$, corresponds to a taper beam of constant thickness. The second geometric dataset are: Length $(L)=360$ mm, thickness $=12$ mm and depth at the fixed end $(h_2)=20$ mm, depth at free end $(h_1)=6$ mm,

Table 1
Comparison of natural frequencies of cantilever beams without crack

α	γ	Analytical (Hz)						Finite element method (Hz)		
		ω_1	p_1	ω_2	p_2	ω_3	p_3	ω_1	ω_2	ω_3
0.4	0.5	61.21	2.7246	276.01	5.7856	688.43	9.1372	61.18	275.11	686.81
0.3	0.2	147.23	3.6594	505.90	6.7834	1224.85	10.5549	147.01	503.55	1210.63
0.5	0.4	102.32	2.6256	450.88	5.5116	1189.64	8.9527	102.22	448.28	1173.42
0.4	0.0	324.39	3.1361	1442.03	6.6121	3630.19	10.4910	322.83	1415.36	3486.97
0.3	0.0	233.73	3.6886	952.01	7.4443	2324.16	11.6315	233.09	940.28	2262.14

length of taper section = 288 mm and length of uniform section = 72 mm. The height truncation factor, α, is 0.3 and length truncation factor, γ, is 0.2. The material data employed are: density $\rho = 7860\ \mathrm{kg/m^3}$, Poisson's ratio = 0.3 and modulus of elasticity $E = 210$ GPa.

The solution to the characteristic equation $|H| = 0$ gives the natural frequencies. The equation has been solved here by the Newton–Raphson method to determine the natural frequencies. The tolerance on the convergence is kept as 10^{-8}. It is observed that an inclusion of the first 20 to 25 terms in the series (Eqs. (13), (14), (17) and (18)) is sufficient for the convergence and good accuracy.

4.1.1. Uncracked beam

The overall beam dimensions conform to the above sizes in all cases. Some cases of (single segment) taper beams have also been examined. For an uncracked beam, $[H]$ is an 8×8 matrix for a two segment beam. A comparison with analytical solutions, wherever possible, and finite element results are presented in Table 1 for the case of two segment cantilever beams. The finite element results are based on a package developed in-house (Maiti, 1996). In all cases, 8-noded subparametric elements (Bathe, 1990) are used for the discretisation. There are 1629 nodes and 500 elements; the element size around the crack tip is kept in the range 8 to 30% of crack length. In the computation, 9-point Gauss quadrature is employed throughout. The agreement with the finite element results is very good, the maximum difference being less than 4%. For purely taper beams, i.e. $\gamma = 0$, which can be treated as special cases of two segment beams, the present results agree exactly with those obtained by Naguleswaran (1994).

Table 2
Comparison of frequency coefficients p for simply supported beams without crack

α	γ	Frobenius Method			Reference results [Auciello and Ercolano 1997]		
		p_1	p_2	p_3	p_1	p_2	p_3
0.1	0.0	6.2366	13.4624	20.0029	6.2366	13.4623	20.0028
0.2	0.0	4.9597	10.3307	15.4081	4.9597	10.3307	15.4081
0.1	0.2	4.1676	11.7968	16.6741	4.1675	11.7968	16.6742
0.2	0.2	4.0491	9.3114	13.8224	4.0492	9.3117	13.8225
0.1	0.4	3.2940	9.4122	14.6626	3.2939	9.4123	14.6626
0.333	0.4	3.4153	7.5838	11.2721	3.4154	7.5839	11.2721

Table 3
Comparison of natural frequencies of cantilever beams with crack

α	γ	β^*	K	Analytical (Hz)			Finite element method (Hz)		
				ω_1 [a]	ω_2 [a]	ω_3 [a]	ω_1	ω_2	ω_3
0.4	0.5	0.2	40.0	61.14	273.68	673.11	61.11	272.84	669.02
		0.35	40.0	60.70	269.48	982.94	60.10	262.03	670.90
		0.75	120.0	60.02	275.64	686.91	60.14	273.03	686.35
		0.75	65.0	59.07	275.35	678.66	59.27	271.34	685.96
0.3	0.2	0.15	57.0	147.12	502.19	1203.79	146.63	498.15	1185.73
		0.15	19.3	146.89	495.83	1165.45	146.41	491.53	1148.68
		0.4	150.0	146.49	495.41	1212.99	145.58	494.31	1206.42
		0.5	120.0	146.12	492.88	1195.71	144.80	497.91	1189.53

[a] ω to p conversion factors: $p_i^2 = 0.1212731\ \omega_i$ (for $\alpha = 0.4$) and $0.0909548\ \omega_i$ (for $\alpha = 0.3$), $i = 1, 2, 3$.

The characteristic equation for simply supported beams can be easily obtained. For certain combinations of height, truncation factor α and length truncation factor γ, which gives the location of the junction of two beam segments, the characteristic equation has been solved to facilitate a comparison with those due to Auciello and Ercolano (1997). The comparison (Table 2) indicates an excellent agreement.

4.1.2. Cracked beam

In the case of a beam with a crack (Ostachowicz and Krawczuk, 1991), the rotational spring stiffness is obtainable from

$$K_t = \frac{bh^2E}{72\pi(a/h)^2 f(a/h)}, \tag{38}$$

where

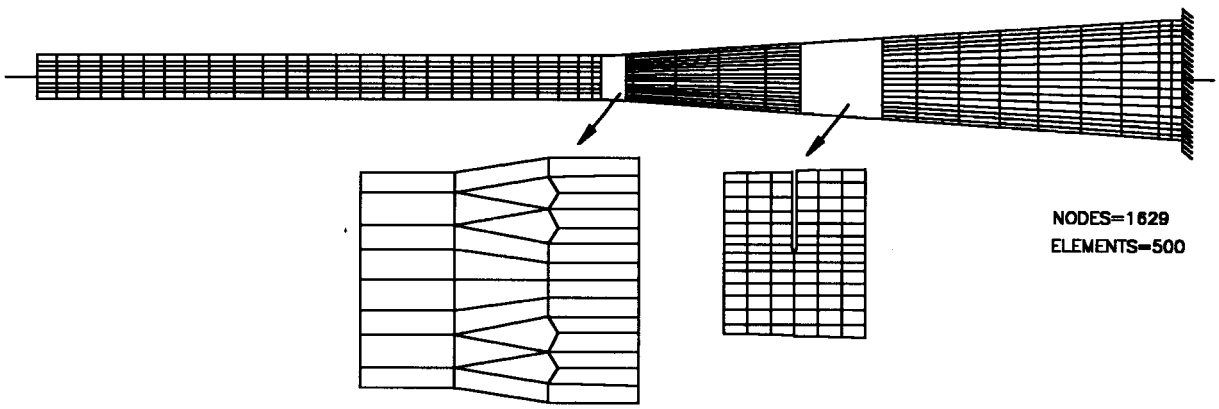

Fig. 2. Typical finite element discretisation.

Table 4
Comparison of actual and predicted crack location and size for cantilever beams ($\alpha = 0.4$)

Actual		Natural frequencies (Hz)			Predicted				
Location size		ω_1 [a]	ω_2 [a]	ω_3 [a]	Location		Stiffness K	Size	
β^*	a (mm)				β^*	% Error		a (mm)	% Error
Crack in uniform section of a beam ($\gamma = 0.5$)									
Uncracked		61.18	275.11	686.81					
0.2	3.0	61.11	272.84	669.02	0.198	−0.2	40.0	2.90	−3.33
0.2	4.0	61.03	270.21	650.59	0.193	−0.7	18.0	3.93	−1.75
0.35	4.0	60.10	262.03	670.90	0.345	−0.5	18.5	3.89	−2.75
0.4	3.0	60.39	268.78	685.11	0.390	−1.0	40.0	2.90	−3.33
0.4	4.0	59.51	262.27	684.08	0.395	−0.5	18.5	3.89	−2.75
Crack in taper section of a beam ($\gamma = 0.5$)									
0.5	3.0	59.61	271.74	678.03	0.508	0.8	117.5	2.97	−1.00
0.5	4.0	57.89	268.23	669.79	0.505	0.5	56.0	4.22	−5.50
0.7	3.76	60.18	274.28	683.52	0.69	−1.0	125.0	3.67	−2.39
0.7	4.90	59.36	273.03	680.91	0.695	−0.5	70.0	4.89	−0.20
0.7	6.40	57.61	272.22	675.41	0.698	−0.2	35.0	6.76	5.62
0.75	4.14	60.14	273.03	686.35	0.73	−2.0	120.0	3.90	−5.79
0.75	5.42	59.27	271.34	685.96	0.74	−1.0	65.0	5.20	−4.05
0.75	7.0	57.53	268.13	682.20	0.744	−0.6	30.0	7.60	8.57
0.8	4.51	60.11	271.38	686.09	0.83	3.0	110.0	4.25	−5.76
0.8	5.94	59.19	268.33	685.78	0.825	2.5	75.0	5.16	−13.13
0.8	7.6	58.76	263.02	685.23	0.83	3.0	40.0	6.98	−8.15
One segment taper beam ($\gamma = 0.0$)									
Uncracked		322.83	1415.36	3486.97					
0.167	1.0	322.82	1413.47	3474.91	0.175	0.8	300.0	1.08	8.00
0.167	2.0	322.72	1409.42	3438.85	0.177	1.0	110.0	1.78	−11.00
0.167	3.08	322.61	1401.29	3369.86	0.177	1.0	42.3	2.88	−6.49
0.167	3.83	322.47	1391.76	3295.07	0.177	1.0	28.7	3.47	−9.39
0.167	5.0	322.08	1366.62	3155.94	0.178	1.1	14.0	4.74	−5.20
0.33	1.2	322.55	1402.95	3448.26	0.34	1.0	310.0	1.14	−5.00
0.33	2.0	322.15	1391.79	3432.13	0.34	1.0	115.0	1.90	−5.00
0.33	3.67	320.63	1349.32	3373.32	0.327	−0.3	28.3	3.85	4.90
0.33	4.67	318.99	1308.46	3321.45	0.330	0.0	16.7	4.89	4.71
0.33	6.0	315.35	1229.17	3231.24	0.333	0.3	8.80	6.35	5.83
0.5	1.4	322.02	1403.36	3454.07	0.505	0.5	270.0	1.32	−5.71
0.5	2.0	321.28	1397.52	3450.19	0.505	0.5	142.5	1.83	−8.50
0.5	4.26	315.93	1357.18	3434.24	0.505	0.5	28.0	4.19	−1.64
0.5	5.50	310.49	1320.40	3399.57	0.505	0.5	15.3	5.54	−0.72
0.5	7.0	300.14	1259.09	3358.20	0.506	0.6	7.80	7.32	4.57
0.67	1.6	321.22	1408.64	3440.24	0.676	0.6	238.0	1.51	−5.62
0.67	2.0	320.40	1408.33	3431.69	0.675	0.5	154.5	1.87	−6.50
0.67	4.8	309.17	1404.32	3318.43	0.675	0.5	25.0	4.75	−1.04
0.67	6.34	298.37	1400.39	3218.71	0.675	0.5	13.0	6.42	1.26
0.67	8.0	280.68	1394.01	3070.23	0.675	0.3	6.80	8.38	4.75

[a] ω to p conversion factors: $p_i^2 = 0.1212731\ \omega_i$ (for $\gamma = 0.5$) and $0.0303182\ \omega_i$ (for $\gamma = 0.0$), $i = 1, 2, 3$.

Table 5
Comparison of actual and predicted crack location and size for cantilever beams ($\alpha = 0.3$)

Actual		Natural frequencies (Hz)			Predicted				
Location size		ω_1 [a]	ω_2 [a]	ω_3 [a]	Location		Stiffness K	Size	
β^*	a (mm)				β^*	% Error		a (mm)	% Error
Crack in uniform section of a beam ($\gamma = 0.2$)									
Uncracked		147.01	503.55	1210.63					
0.1	1.2	146.99	502.92	1206.44	0.122	2.2	260.0	0.893	−25.58
0.1	1.98	146.72	500.98	1199.02	0.11	1.0	75.0	1.65	−16.66
0.1	3.0	146.68	498.97	1184.46	0.105	0.5	24.0	2.66	−11.33
0.15	1.2	146.96	502.06	1201.69	0.15	0.0	163.0	1.13	−5.83
0.15	1.98	146.63	498.15	1185.73	0.1502	0.02	57.0	1.87	−5.55
0.15	3.0	146.41	491.53	1148.68	0.15	0.0	19.3	2.88	−4.00
0.2	1.2	146.89	500.66	1199.34	0.2	0.0	161.7	1.13	−5.83
0.2	1.98	146.48	493.95	1177.93	0.198	−0.2	58.2	1.85	−6.56
0.2	3.0	145.79	479.91	1131.78	0.2	0.0	20.3	2.83	−5.66
Crack in taper section of a beam ($\gamma = 0.2$)									
0.4	0.95	146.82	502.50	1210.26	0.4	0.0	1166.67	0.772	−18.73
0.4	2.58	145.58	494.31	1206.42	0.4	0.0	150.0	2.23	−13.56
0.4	3.46	144.48	487.71	1205.15	0.4	0.0	80.0	3.06	−11.56
0.4	4.73	141.67	472.15	1202.15	0.4	0.0	35.0	4.50	−4.86
0.5	1.12	146.73	503.01	1208.35	0.5	0.0	985.0	0.918	−18.03
0.5	3.15	144.80	497.91	1189.53	0.5	0.0	120.0	2.71	−13.96
0.5	4.22	143.01	494.44	1173.83	0.5	0.0	62.0	3.77	−10.66
0.5	5.61	139.02	487.05	1142.73	0.5	0.0	29.0	5.38	−4.09
0.6	1.29	146.61	503.67	1207.58	0.5	0.0	850.0	1.06	−17.02
0.6	3.72	143.88	501.55	1181.56	0.6	0.0	100.0	3.19	−14.24
0.6	4.97	141.31	501.13	1159.06	0.6	0.0	50.0	4.52	−9.05
0.6	6.48	136.23	500.32	1118.43	0.602	0.2	25.0	6.24	−3.70
One segment taper beam ($\gamma = 0.0$)									
Uncracked		233.09	940.28	2262.14					
0.4	3.29	231.16	911.09	2260.46	0.4	0.0	75.0	2.72	−17.12
0.4	4.39	229.16	886.46	2258.95	0.4	0.0	40.0	3.71	−15.48
0.4	5.80	224.95	839.25	2255.93	0.4	0.0	20.0	5.10	−15.16
0.5	3.74	229.25	918.23	2236.18	0.5	0.0	63.0	3.15	−14.77
0.5	4.99	225.75	899.65	2215.66	0.5	0.0	31.5	4.42	−11.42
0.5	6.50	218.78	866.37	2180.29	0.5	0.0	15.5	6.07	−6.61
0.6	4.19	226.99	932.31	2192.04	0.61	1.0	56.0	3.51	−16.22
0.6	5.59	221.58	925.49	2137.86	0.61	1.0	28.0	4.93	−11.00
0.6	7.20	211.78	913.60	2053.12	0.61	1.0	14.2	6.68	−7.22

[a] ω to p conversion factors: $p_i^2 = 0.0909548\ \omega_i$ (for $\gamma = 0.2$) and $0.0582111\ \omega_i$ (for $\gamma = 0.0$) $i = 1, 2, 3$.

$$f(a/h) = 0.6384 - 1.035(a/h) + 3.7201(a/h)^2 - 5.1773(a/h)^3 + 7.553(a/h)^4 - 7.332(a/h)^5 + 2.4909(a/h)^6, \tag{39}$$

where b and h are the beam thickness and depth, respectively. A higher order polynomial form for $f(a/h)$ can be obtained using more terms of the polynomial expression for the stress intensity factor correction factor, given by Anifantis and Dimarogonas (1983). This is given below

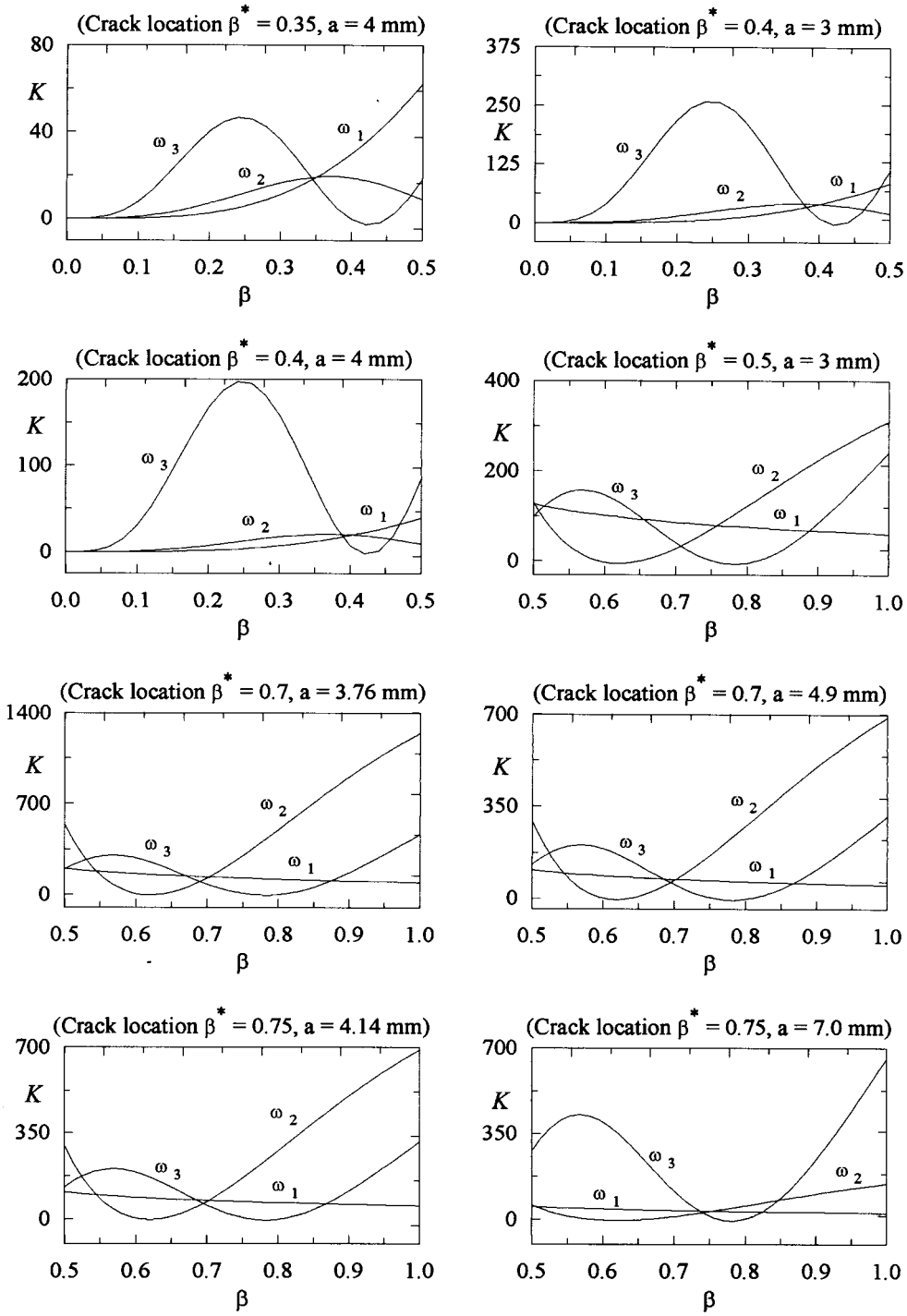

Fig. 3. Plots of stiffness vs. crack location for $\alpha = 0.4$ and $\gamma = 0.5$.

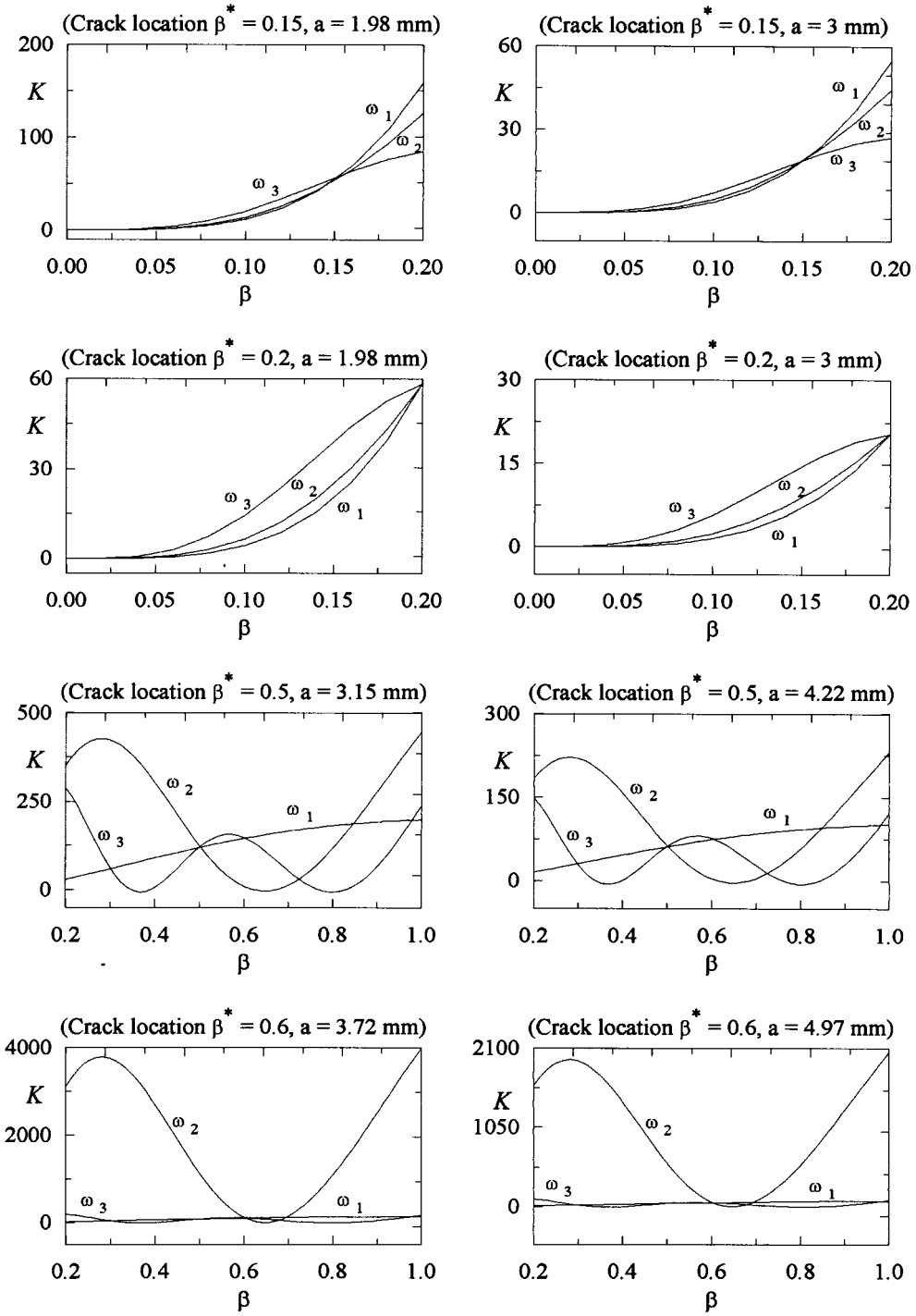

Fig. 4. Plots of stiffness vs. crack location for $\alpha = 0.3$ and $\gamma = 0.2$.

Table 6
Equivalent length of beams for crack size computation

Actual		Total beam length (mm)	Uniform section length (mm)	Taper section length (mm)	Equivalent length (mm)	f_s
α	γ					
0.4	0.5	480.0	240.0	240.0	807.88	1.6831
0.4	0.0	240.0	0.0	240.0	296.88	1.2370
0.3	0.2	360.0	72.0	288.0	542.88	1.5080
0.3	0.0	288.0	0.0	288.0	378.23	1.3133

$$f(a/h) = 0.6384 - 1.035(a/h) + 3.7201(a/h)^2 - 5.1773(a/h)^3 + 7.553(a/h)^4 - 7.332(a/h)^5 + 6.799(a/h)^6 - 6.9956(a/h)^7 + 20.094(a/h)^8 - 22.1145(a/h)^9 + 6.93(a/h)^{10} + 16.115(a/h)^{12}. \quad (40)$$

On substitution of this K, the characteristic equation $|H| = 0$ is obtained. $|H|$ is a 12×12 determinant for a two geometrically segmented beam. The natural frequencies have again been obtained by the Newton–Raphson method. The analytical results are compared in Table 3 with our finite element data. The difference is less than 3%.

4.2. Solution of inverse problem — crack detection

Eqs. (36) and (37) can serve as a basis to solve the inverse problems. It is just necessary to measure or compute the first three transverse natural frequencies of the beam with a crack and the corresponding beam without the crack. Using Eq. (36) or Eq. (37) as appropriate for each mode, a variation of K with crack location β is obtained. Since physically there is only one crack, the position where the three curves intersect gives the crack location and the rotational spring stiffness which simulates the crack. In order to get a common intersection point of the three K vs. β curves, it has been shown (Nandwana and Maiti, 1997c) that the modulus of elasticity, E, which serves as an input to Eq. (36) or Eq. (37) for each mode, must be calculated using the zero setting procedure. This makes the computation/measurement of the uncracked beam's natural frequencies compulsory. The crack size is then obtained using the relationship between stiffness K and crack size a, e.g. Eqs. (38)–(40).

The method of solutions has been tested considering 3 to 4 crack sizes and several crack locations. The natural frequencies of the cracked as well as the virgin beams are computed using the finite element program. For discretisation, mostly eight-noded quadrilateral elements are employed (Fig. 2). For smaller crack sizes (10–20% depth), discretisation with about 1811 nodes and 560 elements has been used. The natural frequencies so obtained are given in Tables 4 and 5. The variations of rotational spring stiffness K with crack location β are shown for a few cases in Figs. 3 and 4. It must be emphasized that twenty-five terms in the expansion Eq. (6) are considered in all case studies for evaluating $|\Delta_1|$ and $|\Delta_2|$. Quadruple precision computation has been found to be very useful and is uniformly employed. It is relevant to note here in passing that, during computation on a PC using a FORTRAN77 compiler, by invoking the '-r16' flag, the quadruple precision can be obtained. The intersection of three curves indicates the possible crack position. Whenever the three curves do not intersect at a single point, the centre of gravity of the three pairs of intersection has been taken as the crack location (Nandwana and Maiti, 1997c). From the comparison of results, it is found that the error in the location prediction is never more than 2.5%.

It is relevant to note here that the change in value due to the use of quarter point singularity elements instead of 8-noded subparametric elements (of the size considered here) around the crack tip is less than 0.9% in the first natural frequency and less than 0.5% in the second natural frequency, and it is negligible in the case of the third natural frequency. This effect reduces further as the size of the 8 noded subparametric elements is decreased. Similar observations have been reported by Nandwana (1998).

Since Eq. (38) is mainly valid for a uniform beam, it cannot be directly applied to geometrically segmented beams. It requires some modifications, particularly when the crack is in the taper segment. An idea of an equivalent beam is found to be very useful for the crack size computation. It is assumed that the given beam is equivalent to a uniform beam of depth h_2 and length L_{eq}. This length L_{eq} is computed by equating the free end deflection of the given beam with that of the equivalent uniform beam. The same load is applied at the free end to calculate the displacement in both the cases. Table 6 gives equivalent lengths (L_{eq}) for a number of cases. After obtaining the crack size a from Eq. (34) using all physical dimensions, it is multiplied by the factor (f_s) where

$$f_s = \frac{\text{Equivalent length}}{\text{Actual beam length}}.$$

For the four cases considered, values of f_s are given in Table 6. The crack sizes obtained by this method are shown in Tables 4 and 5. The maximum error in predicting crack size is around 18% for crack sizes greater than 30% depth. In the range of crack sizes of 10–20% of section depth, the maximum error is 25%. The errors without the proposed correction are much higher, as high as 42%. No theoretical justification can be offered at this stage for the improvement due to the correction.

5. Conclusions

A method for modelling transverse vibration of geometrically segmented slender beams has been proposed using the Frobenius method of solving Euler–Bernoulli type differential equations. The case studies involving beams up to two segments have clearly demonstrated the accuracy of the modelling and the usefulness of the method for both the forward and inverse problems. Crack sizes 10–50% of section depth have been examined. The accuracy in the case of the forward problem is excellent. The method can be easily adapted for a number of segments more than two. This will simply increase the size of the characteristic matrix $[H]$. While locating a crack, the method does not involve any iteration and the accuracy for the detection is very encouraging. The crack size can be obtained with errors around 25% using the concept of an equivalent beam length, which is needed to handle a crack in the taper segment of the beam. The equivalent beam length is obtained by equating the free end deflection of the given beam with the free end deflection of a uniform beam of depth equal to the depth at the big end. The same load is considered to be applied at the free end in both cases.

References

Adams, R.D., Walton, D., Flitcroft, J.E., Short, D., 1975. Vibration testing as a nondestructive test tool for composite materials. Composite Reliability ASTM STP 580, 159–175.

Anifantis, N., Dimarogonas, A., 1983. Stability of columns with a single crack subjected to follower and vertical loads. International Journal of Solids and Structures 19, 281–291.

Auciello, N.M., Ercolano, A., 1997. Exact solution for the transverse vibration of a beam, a part of which is a taper beam and other part is a uniform beam. International Journal of Solids and Structures 34, 2115–2129.

Bathe, K.J., 1990. Finite Element Procedures in Engineering Analysis. Prentice Hall of India, New Delhi.

Carnegie, W., Thomas, J., 1967. Natural frequencies of long tapered cantilevers. The Aeronautical Quarterly 18, 309–320.

Cawley, P., Adams, R.D., 1979. The location of defects in structure from measurements of natural frequencies. Journal of Strain Analysis 14, 49–57.

Conway, H.D., Dubil, J.F., 1965. Vibration frequencies of truncated-cone and wedge beams. ASME Journal of Applied Mechanics 32, 932–934.

Dimarogonas, A.D., 1987. Modelling damaged structural members for vibration analysis. Journal of Sound and Vibration 112, 541–543.

Gaines, J.H., Volterra, E., 1966. Transverse vibrations of cantilever bars of variable cross-section. Journal of Acoustical Society of America 39, 674–679.

Liang, R.Y., Choy, F.K., Hu, J., 1991. Detection of cracks in beam structures using measurements of natural frequencies. Journal of the Franklin Institute 328, 505–518.

Mabie, H.H., Rogers, C.B., 1968. Transverse vibrations of tapered cantilever beams with end support. Journal of Acoustical Society of America 44, 1739–1741.

Maiti, S.K., 1996. Finite Element Package for Stress and Vibration Analysis. Mechanical Engineering Department. Indian Institute of Technology, Bombay, pp. 8–74 MED-SKM-TR-96-01.

Martin, A.I., 1956. Some integrals relating to the vibration of a cantilever beam and approximation for the effect of taper on overtone frequencies. The Aeronautical Quarterly 7, 120–128.

Naguleswaran, S., 1994. A direct solution for transverse vibration of Euler–Bernoulli wedge and cone beams. Journal of Sound and Vibration 172, 289–304.

Nandwana, B.P., 1998. On foundation for detection of crack based on measurement of natural frequencies. Ph.D. Thesis, Mechanical Engineering Department, Indian Institute of Technology, Bombay.

Nandwana, B.P., Maiti, S.K., 1997a. Detection of location and size of a crack in stepped cantilever beams based on measurements of natural frequencies. Journal of Sound and Vibration 203, 435–446.

Nandwana, B.P., Maiti, S.K., 1997b. Vibration based detection of location and size of edge crack in beams on multiple supports. In: Proceedings of the 9th International Conference on Fracture. Pergamon Press, Oxford, pp. 2603–2610.

Nandwana, B.P., Maiti, S.K., 1997c. Modelling of vibration of beam in presence of inclined edge and internal crack for its possible detection based on frequency measurements. Engineering Fracture Mechanics 58 (3), 193–205.

Ostachowicz, W.M., Krawczuk, M., 1991. Analysis of the effect of cracks on the natural frequencies of a cantilever beam. Journal of Sound and Vibration 150, 191–201.

Rao, J.S., 1965. The fundamental flexural vibration of a cantilever beam of rectangular cross-section with uniform taper. The Aeronautical Quarterly 16, 139–148.

Rizos, P.F., Aspragathos, N., Dimarogonas, A.D., 1990. Identification of crack location and magnitude in a cantilever beam from the vibration modes. Journal of Sound and Vibration 138, 381–388.

Wang, H.C., 1967. Generalised hypergeometric function solutions on the transverse vibration of a class of non-uniform beams. ASME Journal of Applied Mechanics 34, 702–708.